Iraqi Journal of Physics, 2019 *Vol.17, No.43, PP. 67-76*
DOI: 10.20723/ijp.17.43.67-76

Morphological and optical properties of V_2O_5:TiO_2 thin film prepared by PLD technique

Safaa M. Mahdi[1] and Ghuson H. Mohammed[2]

[1]Oil Products Distribution Company, Ministry of Oil

[2]Department of Physics, College of Sciences, University of Baghdad

E-mail: algodaasafaa@gmail.com

Abstract

In this work, pure and doped Vanadium Pentoxide (V_2O_5) thin films with different concentration of TiO_2 (0, 0.1, 0.3, 0.5) wt were obtained using Pulse laser deposition technique on amorphous glass substrate with thickness of (250) nm. The morphological, UV-Visible and Fourier Transform Infrared Spectroscopy (FT-IR) were studied. TiO_2 doping into V_2O_5 matrix revealed an interesting morphological change from an array of high density pure V_2O_5 nanorods (~140 nm) to granular structure in TiO_2-doped V_2O_5 thin film. Transform Infrared Spectroscopy (FTIR) are used to analyze structural properties of as-deposit. The transmittance and absorption of each film, in the spectral range 300 to 1100 nm, were measured from which the optical constants (Refractive index, Absorption coefficient, Extinction coefficient and Energy gap) were determine d.The energy band gap of the films was found to be change from (2.38 to 2.9) eV when the concentration of TiO_2 increases from (2.78 to 2.9) eV The results showed a significant improvement in the transmittance and refractive index in TiO_2 doped V_2O_5 thin films .All measured values were in consistent with other previous studies.

Key words
Pulsed laser deposition, nanoparticles thin films, structural properties, optical properties.

Article info.
Received: Jun. 2019
Accepted: Jul. 2019
Published: Dec. 2019

الخصائص التركيبية البصرية لاغشية TiO_2:V_2O_5 الرقيقة المحضرة بتقنية الليزر النبضي

صفاء محسن مهدي[1] و غصون حميد محمد[2]

[1]شركة توزيع المنتجات النفطية، وزارة النفط

[2]قسم الفيزياء، كلية العلوم، جامعة بغداد

الخلاصة

في هذا العمل اغشية أوكسيد الفناديوم (V_2O_5) الرقيقة النقية والمشوبة مع تراكيز مختلفة لأوكسيد التيتانيوم (TiO_2) و بالقيم (0, 0.1, 0.3, 0.5) والتي تم تحضيرها بتقنية الليزر النبضي و ترسيبها على سطح زجاجي عشوائي مع سمك (250) نانومتر وتم دراسة خواصها التركيبية بـأستخدام الاشعة فوق البنفسجية (UV) و جهاز تحليل الاشعة تحت الحمراء (FTIR) والذي يستخدم لتحليل الخصائص التركيبية .أوكسيد التيتانيوم االمشوب مع أوكسيد التيتانيوم كشفت عن تغيير في صفوفذات الكثافة العالية لأوكسيد الفناديوم الغير مشوب أنابيب نانوية تساوي تقريبا 140 نانومتر الى تركيب حبيبي لأغشية أوكسيد الفناديوم المشوبة بأوكسد التيتانيوم الرقيقة .جهاز تحليل الأشعة تحت الحمراء يستخدم لتحليل الخصائص التركيبية من النماذج المحضرة. الانتقالية والامتصاصية لكل غشاء عند المدى 300-1100 nm حيث تم قياس الثوابت البصرية (معامل الانكسار، معامل الامتصاص، معامل الخمود، فجوة الطاقة). فجوة الطاقة للاغشية وجدت تتغير من (2.38 الى 2.9) الكترون فولت و مع التشويب بأوكسد التيتانيوم تزداد من (2.78 الى 2.9) الكترون فولت. كل قيم القياس بما يتفق مع غيرها من الدراسات السابقة.

Introduction

The transition metal oxides attract a lot of attention due to their interesting physical, chemical, electronic, and optical properties which arise from the narrow d states as well as their hybridization with the ligand p orbital. The vanadium pentoxide (V_2O_5) has attracted considerable interest owing to their multi valence, layered structure, wide optical band gap, good chemical and thermal stability, and excellent thermoelectric property [1, 2]. Scientific and technological applications of V_2O_5 in thin films form includes electronic and optical switches [3], electro chromic devices [4], window for solar cell [5, 6], microelectronic devices [7], thin film batteries (TFB) [8]. V_2O_5 crystallizes with an orthorhombic unit cell structure and belongs to space group with the lattice parameters a=11.51 Å, b=3.56 Åand c= 4.3Å [9]. V_2O_5 is an indirect semiconductor with a band gap of 2.3-2.4 eV, which stems from the split-off oxygen 2p band up to vanadium 3d band. Electronic conduction in V_2O_5 is highlyanisotropic with conduction within the a-b planes considerably higher than conduction perpendicular to these planes.

Understanding the unique properties of V_2O_5 requires a great structural investigation especially in case of doping the oxide with other elements that may result in a change of morphology, structural arrangement and optical properties of this material. The structural stability of this V_2O_5 doped with guest atoms is also important because small amount of admixtures may strongly affect the reactivity of this oxide. The novel technology of the nanostructure material assembling provides the possibility of tailoring such materials with unique microstructure properties. The proper amount of transition metal doping could lead to optimal degree of nonstoichiometry for better performance. Since composites and mixed phases can have different properties than their constituent phases. Various metals like W, Pd, Mo, Mn have been used to dope the V_2O_5 for several applications like enhanced electrochemical performance, better intercalation property, improved cyclic stability, and various other electronic applications. But doping with Titanium dioxide (TiO_2) may significantly improve the photo catalytic applications of V_2O_5. TiO_2 has been proven to be an effective material for applications such as photocatalysis [10], dye sensitized solar cells [11], self-cleaning/antifogging surface coatings [12], etc. Its photo catalytic activity is normally determined by the particle size [13], phase composition [14], and the position of the conduction and valance bands in the energy scale [15]. In the thin film form, TiO_2 is usually used in photovoltaic applications such as photo electrochemical system (PEC) and dye sensitized solar cell (DSSC) for photon harvesting [16]. Moreover, TiO_2 offers the advantage of energy alignment between the energy position of the valance band edge and the redox species in the electrolyte by potential biasing the photo anodes. This helps to optimize the quantum efficiency. The deviation of stoichiometry suggests that the properties of the films are mainly dependent on the deposition technique and the deposition conditions such as vacuum, deposition temperature, deposition rate, residual gases in the vacuum chamber during deposition, etc. Many research groups have reported work on V_2O_5- TiO_2 composite thin films [17, 18]. These materials have already proved to be promising for the development of the solar energy devices such as counter electrodes for the electro chromic windows and thin film layers for the

antireflective filters. The aim of the present study was to synthesize high quality V_2O_5, TiO_2 and $(V_2O_5)_{1-x}$ $(TiO_2)_x$ composite thin films on glass substrate using pulsed laser deposition technique and to study the effect of TiO2 content on the microstructure and optical properties of V_2O_5. It was observed that doping with TiO_2 significantly promotes the phase transformation in V_2O_5 from anatase to rutile phase with significant change in morphology from a nanorod array to granular structure. The influence of TiO_2 doping on the optical properties of V_2O_5 films was also discussed.

Experimental parts

1. Material preparation

Bulk samples of V_2O_5:TiO_2 have been prepared by solid state reaction process. The powder of V_2O_5 and TiO_2 with a purity of 99.99% are mixed together at a different concentration of (X = 0, 0.1, 0.3, 0.5) wt. % of the formula $(V_2O_5)_{1-x}(TiO_2)_x$ in a mixture machine for (10minute) .After that it is pressed into pellets with (1.2 cm) diameter and (0.2 cm) thick, using hydraulic piston type (SPECAC), under the pressure of 2 tons/cm^2 for 5 minutes. The pellets are sintered in air to temperature (400 ^oC) for 1 hours then cooled to room temperature. The temperature of the furnace is raised at a rate of 250 ^oC/hour. The pulsed laser deposition experiment is fulfilled inside a vacuum chamber under (10^{-3} mbar) vacuum conditions. The focused Nd:YAG laser beam at 600 mJ with a frequency second radiation at 1064 nm (pulse width 9 ns) frequency (6 Hz), for 300 laser pulses incident on the target surface makes an angle of 45° with it. The distance between the target and the laser gun was set to 15 cm, and between the target and the substrate was 2 cm.

2. The measurements

The surface morphological was analysised using AFM type (Scanning probe microscope type AA3000), supplied by the Angstrom Advanced Company to determine the grain size and roughness.The 8000S, SHIMADZU) on the basis scan FTIR In the range between (400-4000) cm^{-1} has been carried out. The purpose of this analysis is to provide more details on production Phase powder and identity. A small amount of powder is mixed with KBr on disc which is transparent. This disc is sandwiched in cell FTIR (NaCl cell) and FTIR spectrum with estimated spectrometer. Optical properties of films with different content of x in $(TiO_2)_x$ was measured and determined at a wavelength of about 400 to 1100 nm using UV/VIS Centra 5 spectrometer that previous GBC Scientific Equipment PTY.

Result and discussion

The surface topography of the films as studied by atomic force microscopy (AFM) revealed that laser ablated $(V_2O_5)_{1-x}$ $(TiO_2)_x$ composite thin films were homogenous, smooth and uniform [Fig.1]. The average value of surface roughness was found to decrease with increasing of the TiO_2 content [Table 1]. The image shows the different grain growth in shape and size with the changing TiO_2 content. The occurrence of the large size particles in our film is due to the incomplete elimination of the crater - like features on the target surface, which is caused by ultra-rapid evaporation of the target material.

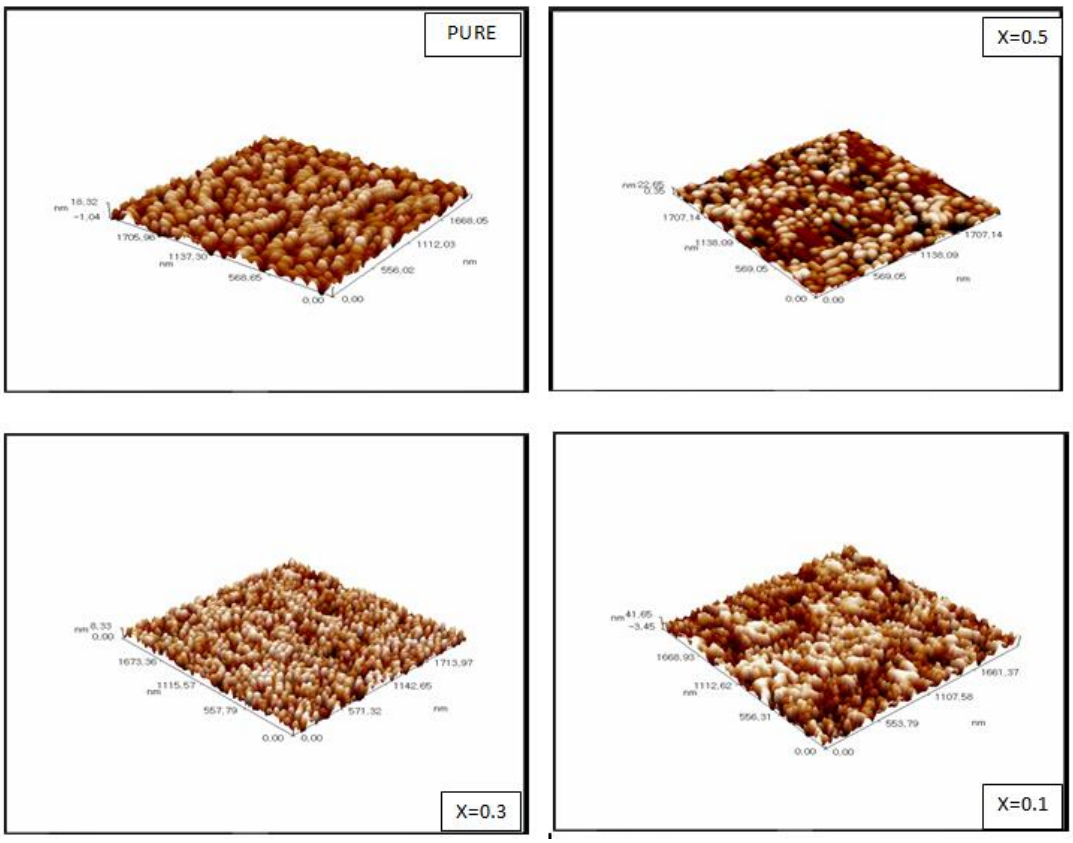

Fig. 1: AFM image for $(V_2O_5)_{1-x}(TiO_2)_x$ films at RT with different TiO_2 content (x=0, 0.1, 0.3, 0.5).

Table 1: Average grain size and average roughness for $(V_2O_5)_{1-x}(TiO_2)_x$ films with different TiO_2 content at R.T.

TiO_2%	RMS Roughness (nm)	Ave. grain size (nm)	Ave. Roughness (nm)
0	13.00	104.37	11.20
0.1	6.46	88.31	5.62
0.3	4.52	80.83	3.78
0.5	2.41	64.90	2.09

FTIR analysis for V_2O_5:TiO_2 own in Figs. 2 show The characteristic peaks of vanadium oxide for V_2O_5 appear at 1037, 607 and 486 cm^{-1} are corresponding to the stretching vibration of terminal oxygen bonds (V=O), the vibration of doubly coordinated oxygen (bridge oxygen) bonds and the asymmetric and symmetric stretching vibrations of triply coordinated oxygen (chain oxygen) bonds, respectively. This spectrum shows two sharp peaks between 3417 and 3448 cm^{-1}, In the FTIR spectrum for the vanadium oxide hexadecylamine composites, the sharp peaks between 3300 and 3500cm^{-1} disappear while the peaks at 2931 and 1550 cm^{-1} are observed. These are assigned to the stretching vibration and asymmetric bending vibration. In comparison with the FTIR spectrum for the vanadium oxide-hexadecylamine composite ,the peak at 1550 cm^{-1} has not shifted while the peak at 1514 cm^{-1} is shifted to 1527 cm^{-1}, which can be associated with the strength change of hydrogen bonding from hydrothermal treatment [19]. The signals between 422 and 1037 cm^{-1} in Fig.2 can be

attributed to various (group) vibrations of V-O type. The vanadium oxide-hexadecylamine composite exhibits intense absorption bands at 514, 632, 773,945 and cm^{-1}. Incontrast, the vanadium. Oxide nanotubes have only two intense peaks at 991 cm^{-1}. Smaller peaks are observed at 607cm^{-1}. The signal at 833 cm^{-1}, which was intense before the hydrothermal reaction, has almost disappeared in the spectrum from nanotubes. This large difference in the range of the V-O vibrations of the samples before and after hydrothermal treatments clearly gives evidence that during the hydrothermal treatment a considerable rearrangement of the vanadium oxide structure takes place, which results in the transformation of the lamellar vanadium oxide amine composite to the nanotubes .It is known that V_2O_5 displays three major absorption peaks at 607, 831 and 1018 cm^{-1}. The absorption at about 999 cm^{-1} is associated with the V=O band. So the band at 991 cm^{-1} in the FTIR spectrum of the vanadium oxide nanotubes and the one at 945 cm^{-1} in the vanadium oxide-hexadecylamine composite belong to the V=O vibration, i.e., the vanadyl group seems to be very much influenced by hydrothermal reaction. In the V_2O_5 spectra the peaks at 636 and 854 cm^{-1} are assigned to the vibrations of V-O-V and O-(V)3, respectively. These signals can be observed at 684 cm^{-1}, respectively, in the spectrum of vanadium oxide-hexadecylamine composite while they do not have corresponding peaks in the spectrum of vanadium oxide nanotubes.

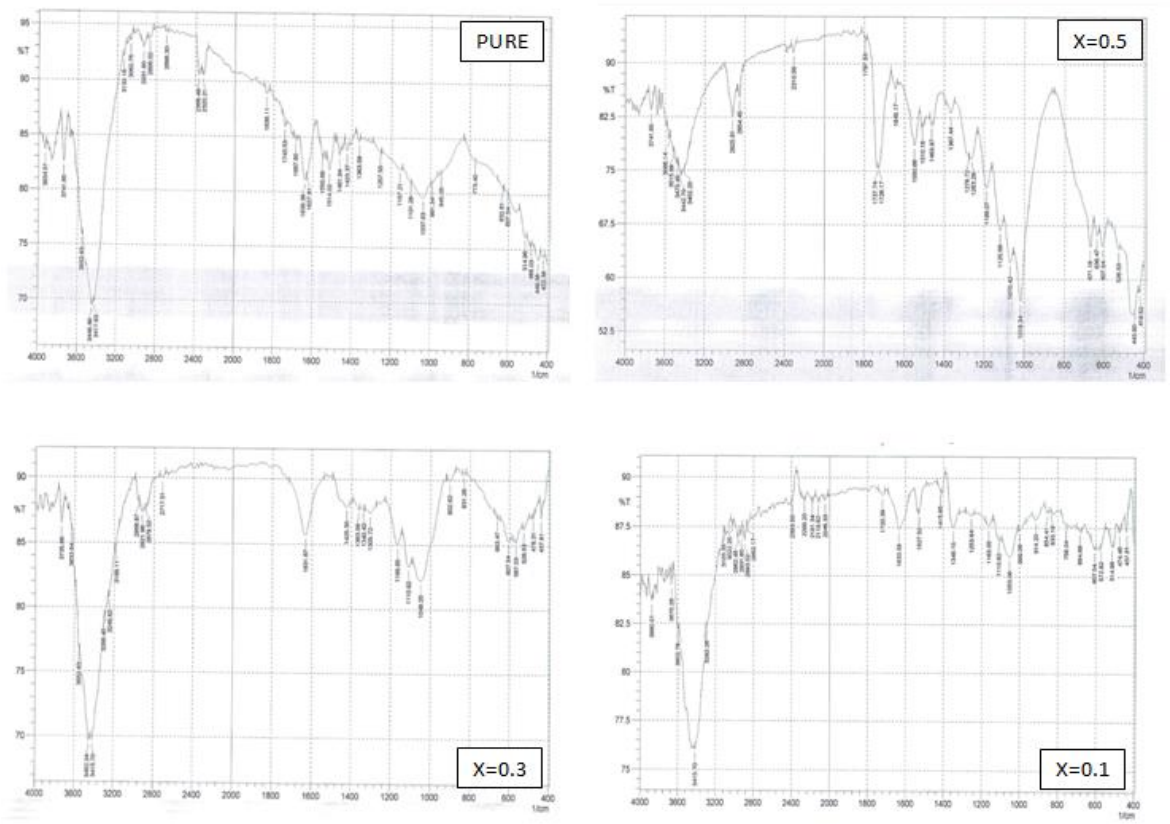

Fig. 2: FTIR pictures for $(V_2O_5)_{1-x}(TiO_2)_x$ films at RT with different TiO_2 content (x =0, 0.1, 0.3, 0.5).

Optical properties

The transmittance

Fig.3 shows the transmittance spectrum as a function of wavelength in the range of (350-1100) nm of V_2O_5:TiO_2 thin films deposited at room temperature with different TiO_2 content (X= 0, 0.1, 0.3 and 0.5). It is obvious from this figure that the transmittance is proportional to concentration it increases with the increasing of TiO_2 content. In the visible range, transmittance is higher than 70 % for sample of X=0.3. Increase in TiO_2 content leads to increase in transmittance. At X=0 (pure V_2O_5), films show transmittance up to 40% in the visible range of electromagnetic spectrum. Lack of oscillations suggests that the films so formed are very thin. At X=0.1 the transmittance is 70 %. With the incorporation of TiO_2 there is gradual increased in transmittance as addition of TiO_2 leads to transparency of films which in turn leads to increases in transmittance results we conclude that this films is very appropriate in the solar cell applications.

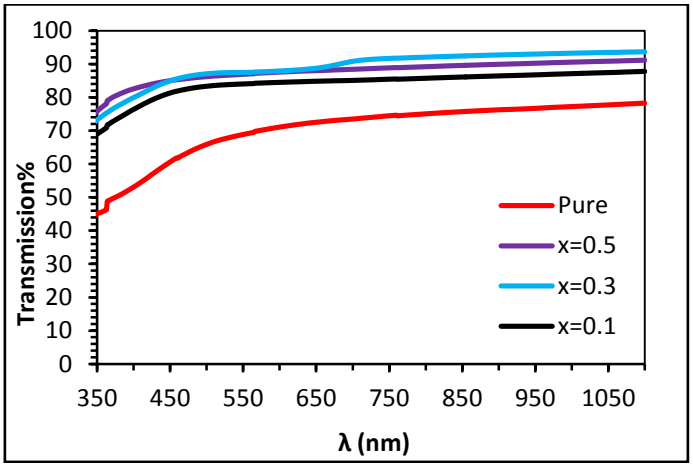

Fig. 3: Optical transmittance for V_2O_5:TiO_2 at R.T.

The energy gap

Fig. 4 shows the variation of $(\alpha h\gamma)^2$ as afunction of $(h\gamma)$ for V_2O_5 doped TiO_2 .By using Tauc equation $(\alpha h\upsilon=Bh\upsilon-E_g]^r)$ to determine the values of the optical energy band gap (E_g) for V_2O_5 films for plotting the relations $(\alpha h\gamma)^r$ versus photon energy $(h\upsilon)$ and select the optimum linear part. It is found that the relation for r=2 yields linear dependence, which indicates the allowed direct transition. The optical energy band gap (E_g) of the films is calculated from the linear part of the plots of $(\alpha h\gamma)^2$ versus photon energy $(h\gamma)$ to α= 0. The optical bandgap of the films can be evaluated from extrapolating the linear portion to the axis. The values of optical energy gap increases with increasing of TiO_2 content, due to decrease in the absorption and increases in the transmission. E_g increases from 2.38 eV to 2.9 eV with increasing the TiO_2 content from 0.1 to 0.5, respectively as shown in the Table 2.

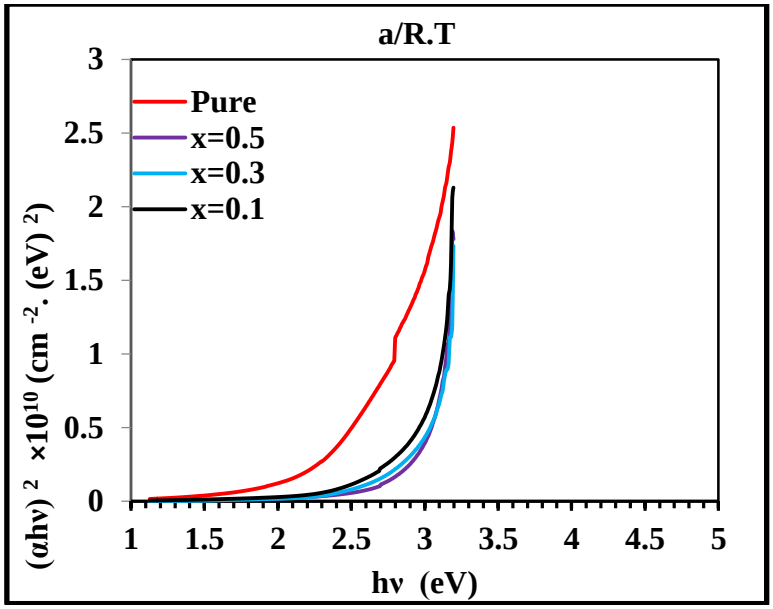

Fig. 4: Optical energy gap for V_2O_5:TiO_2 at R.T.

Table 2: illustrate the values of Egopt and optical constants at λc=520 nm for $(V_2O_5)_{1-x}(TiO_2)_x$ films with different TiO_2 content at R.T.

T_a (˚c)	TiO_2%	T%	α*10^4 (cm^{-1})	K	n	ε_r	ε_i	direct E_g^{opt}(eV)
RT	0	67.327	1.582	0.0655	2.298	5.278	0.3010	2.38
	0.1	83.715	0.710	0.0294	1.827	3.339	0.1070	2.78
	0.3	86.54	0.578	0.023	1.732	3.000	0.0829	2.87
	0.5	87.336	0.540	0.022	1.703	2.900	0.0760	2.90

The refractivity

The variation of the refractive index with wavelength in the range (350–1100) nm for $(V_2O_5)_{1-x}(TiO_2)_x$ films with different concentrations of TiO_2 at room temperature is illustrated in Fig.5. In general, it can be noticed from this figure that the refractive index decreases with increasing the concentration of TiO_2. This can be connected with the decreases in the size of the grains. The values of refractive index are given in Table 2.

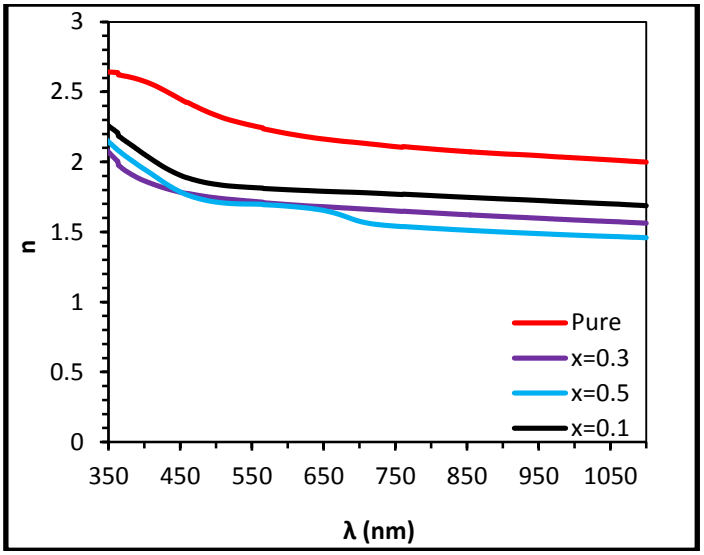

Fig.5: Optical refractive index for V_2O_5:TiO_2 at R.T.

The extinction coefficient

The extinction coefficient was calculated using equation K=αλ/4π. Fig.6 shows the variation of the extinction coefficient as a function of wavelength in the range (350–1100) nm for $(V2O_5)_{1-x}(TiO_2)_x$ films with different concentrations of TiO_2 at room temperature .It can be noticed from these figures that in general the changes of the extinction coefficient follow the same changes of the absorption coefficient with the increasing of TiO_2 concentration. The value of extinction coefficient at different TiO_2 content is shown in Table 2.

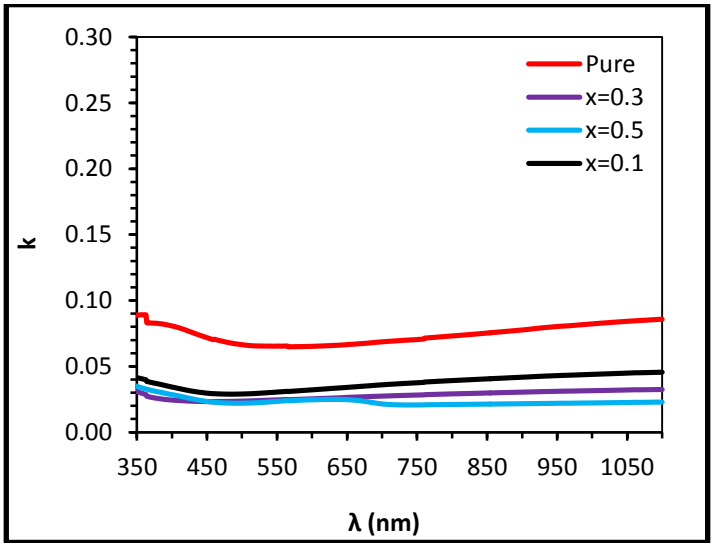

Fig. 6: Optical Extinction Coefficient for V_2O_5:TiO_2 at R.T.

Optical dielectric constant measurements

The variation of the real and imaginary parts of the dielectric constant values with wavelength in the range (350–1100) nm for (for $(V_2O_5)_{1-x}(TiO_2)_x$ films with different concentrations of TiO_2 at room temperature are shown in Figs. 7, respectively. The behavior of E_r is similar to that of the refractive index because of the smaller value of k^2

compared with n^2 according to equation ($Er=k^2-n^2$), while E_i depends mainly on the k values.

The imaginary part of the dielectric constant E_i shows the revers behavior of E_r with the variation of TiO_2 content at λ=520 nm. It is clear from Table 2 that E_i and E_r for $(V_2O_5)_{1-x}(TiO_2)_x$ films decreases when TiO_2 content increases. The values of the dielectric constants ($_r$ and $_i$) at different concentrations of TiO_2 for $(V_2O_5)_{1-x}(TiO_2)_x$ thin film at λ=520 nm are shown in Table 2.

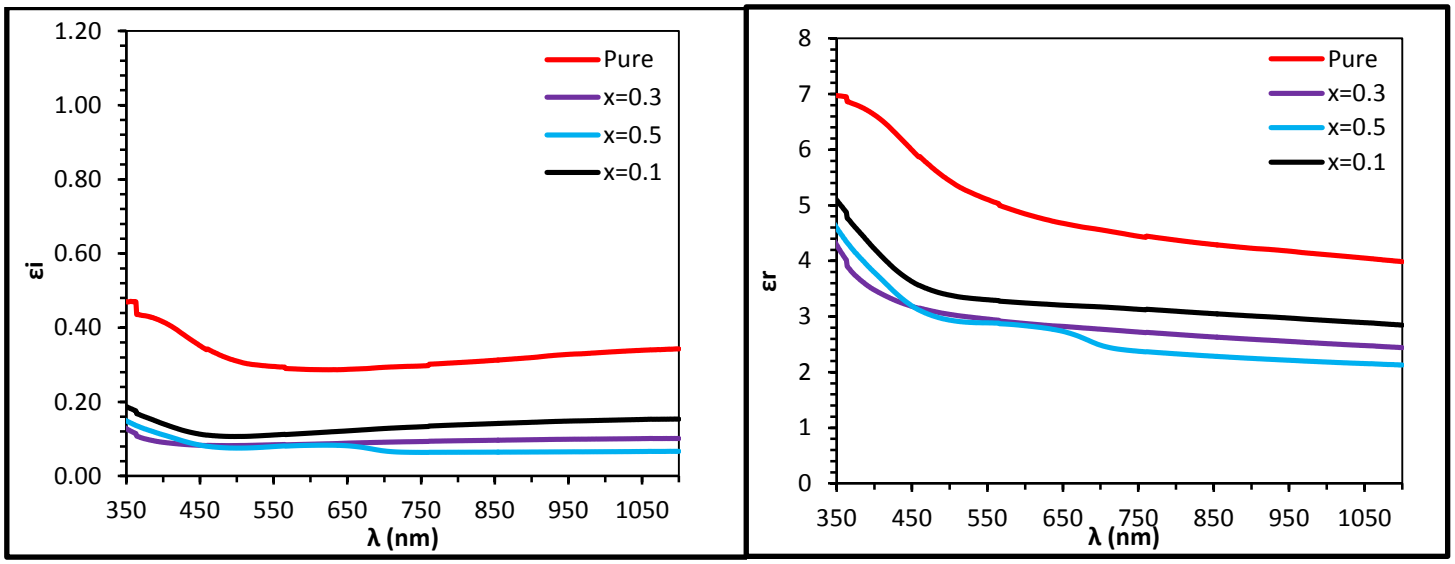

Fig. 7: Optical constant for V_2O_5:TiO_2 at R.T.

Conclusion

In this work, we have successfully prepared un-doped and doped V_2O_5 with different concentration of TiO_2 films on glass, Si substrate by PLD method. The resulting films were characterized by XRD measurements prove that the amorphous structure form of V_2O_5. AFM images of all samples are displayed granular structure. The granular films show higher surface area. Decreasing in grains size with increasing of doping concentration ratio of TiO_2. Un-doped and doped V_2O_5 films demonstrate more than 70 % transmittance at wavelengths longer than 550 nm. Optical energy gap variation between (2.38 eV- 2.90 eV) for TiO_2 doping at R.T.

References

[1] CV. Ramana, OM. Hussain, NB. Srinivasalu, C. Julien, M. Balkanski, Mater SciEng B., 52, 1 (1998) 32-39.
[2] AZ. Moshfegh, Thin Solid Films, 198, 1-2 (1991) 251-268.
[3] RJ. Colton, AM. Guzman, JW. Rabalais, J. Appl. Phys., 49 (1978) 409-416.
[4] Y. Wei, J. Zhou, J. Zheng, C. Xu, Electrochim Acta., 166 (2015) 277-284.
[5] SN. Alamria, AA. Joraid, Materials Science Forum., 663-665 (2011) 743-750.
[6] FN. Dultsev, LL. Vasilieva, SM. Maroshina, LD. Pokrovsky, Thin Solid Films, 510, 1-2 (2006) 255-259.
[7] RB. Darling, S. Iwanaga, Sadhana, 34, 4 (2009) 531-542.
[8] E. Armstrong, D. McNulty, H. Geaney, C. O'Dwyer, ACS Appl. Mater. Interfaces, 7, 48 (2015) 27006-27015.
[9] YS. Yoon, JS. Kim, SH. Choi, Thin Solid Films, 460, 1-2 (2004) 41-47.
[10] K. Nakata, A. Fujishima, J. Photochem. Photobiol, C. 13, 3 (2012) 169-189.

[11] J. Fan, Z. Li, W. Zhou, Y. Miao, Y. Zhang, J. Hu, G. Shao, Appl Surf Sci., 319 (2014) 75-82.
[12] Y. Lai, Y. Tang, J. Gong, D. Gong, L. Chi, C. Lin, Z. Chen, J. Mater. Chem., 22 (2012) 7420-7426.
[13] Z. Tan, K. Sato, S.Takami, RSC Adv., 3 (2013) 19268-19271.
[14] Balázs Réti, Zoltán Major, Dóra Szarka, Tamás Boldizsár, Endre Horváth, Arnaud Magrez, László Forró, A. Dombi, K. Hernádi, J. Mol. Catal A: Chem., 414 (2016) 140-147.
[15] H. Yan, X. Wang, M. Yao, X. Yao, Progress in Natural Science: Materials International, 23, 4 (2013) 402-407.
[16] SK. Deb, Solar Energy Materials & Solar Cells, 88 (2005) 1-10.
[17] S. Kim, M. Taya, Solar Energy Materials and Solar Cells, 107 (2012) 225-229.
[18] V. Goyal, V_2O_5 Composite thin fims Fabrication and Characterization, (2012).
[19] D. R. W. Briigel, "An Introduction to Infrared Spectroscopy" (New York, 1962) p. 165.